"A Cochlear Nucleus Auditory prosthesis based on microstimulation"

Contract No. **No. NO1-DC-4-0005**

Progress Report #5

HUNTINGTON MEDICAL RESEARCH INSTITUTES

NEURAL ENGINEERING LABORATORY

734 Fairmount Avenue

Pasadena, California 91105

D.B. McCreery, Ph.D.

L.A. Bullara, B.S.

A.S. Lossinsky, Ph.D.

HOUSE EAR INSTITUTE

2100 WEST THIRD STREET

Los Angeles, California 90057

R.V. Shannon Ph.D

S. Otto M.S.

M. Waring, Ph.D

ABSTRACT

One goal of this project is to develop arrays of multisite silicon substrate electrodes, which should allow placement of many more microstimulating sites within the human cochlear nucleus than is possible with discrete iridium microelectrodes. We are developing arrays for implantation into the human cochlear nucleus that have 16 electrode sites distributed on 4 silicon shanks extending from an epoxy superstructure that is 2.4 mm in diameter.

Here we report data from a terminal experiment conducted in a cat in which the microstimulating array had been implanted in the cochlear nucleus for 195 days. Using multi-channel recording of neuronal activity in the central nucleus of the inferior colliculus (ICC), we have begun to evaluate the capacity of our intranuclear microstimulating arrays to access separate neuronal population in the feline cochlear nucleus, over a range of stimulus amplitudes. Multiunit neuronal activity was recorded in the central nucleus of the contralateral ICC using a 32-site silicon substrate probe. We generated post-stimulus time (PST) histograms of the neuronal activity that was recorded at each of 16 sites in the ICC and then generated contour ("topographic") maps of the evoked neuronal activity from the set of 16 PST histograms. The full range of responses was seen best in the recordings from the rostral inferior colliculus. Current source-sink density analyses also were performed for each set of 16 simultaneously-recorded templates of the averaged evoked potentials.

Even at the highest stimulus amplitude used, (30 μA) adjacent microstimulating sites in the medial part of the CN separated by only 300 μm induced neuronal activity in largely non-overlapping regions along the dorsolateral-ventromedial axis ICC. Overall, the neuronal activity evoked in the IC from the different sites in the CN was consistent with the known tonotopic distribution of the auditory nerve fibers in the ventral CN (e.g., Leake and Snyder, 1989). The current density analyses gave similar results, and showed the same relation between depth of activity in the ICC and location of the simulation sites in the CN as did the unit activity. However, when the maximum response was in the ventral or the ventromedial IC (corresponding to high or medium

acoustic frequencies) the maxima of the current sinks were 200 to 300 μm shallower (more dorsolateral) in the IC than the maximum multiunit activity. This shift could be an artifact of the multi-site recording probe, These are quite broad at the top and taper towards the tip, and the multiunit activities from the sites that are closer to the tip (deeper in the IC) tend to have better signal-to-noise ratios. This would cause the centroids of the maps of the density of the multiunit activity to be shifted deeper in the ICC, since only neuronal units with S/N greater than 3.5 x the RMS noise level were counted.

1: Development of a multi-site silicon-substrate microstimulating array

INTRODUCTION

The workscope of our contract calls for the development of arrays of silicon substrate electrodes, which should allow placement of many more electrode sites into the human cochlear nucleus than is possible with discrete iridium microelectrodes. We are developing arrays for implantation into the human cochlear nucleus that have 16 electrode sites distributed on 4 silicon shanks extending from an epoxy superstructure that is 2.4 mm in diameter. This is the same footprint as our first-generation human arrays employing discrete iridium microelectrodes and it is designed to be implanted using the same inserter tool.

We have been conducting animal studies using microstimulating arrays with silicon substrate probes fabricated at the University of Michigan under the direction of Design Engineer Jamille Hetke. Figure 1A shows a probe with 2 shanks and 8 stimulating sites, that have been sputter-coated with iridium oxide. The 4 sites on each shank are 0.8mm to 1.7 mm below the top of the shanks. Figure 1B shows an array containing 2 of the probes (4 shanks and 16 electrode sites) extending from an epoxy superstructure that floats of the surface of the cochlear nucleus. The cable is angled vertically, to accommodate the trans-cerebellar approach to the feline cochlear nucleus.

In principle, the silicon substrate array could provide improve functionality of a central auditory prosthesis by affording highly localized stimulation of neuronal populations within the ventral cochlear nucleus (VCN). In theory, this localized stimulation should allow precise and selective access to the tonotopic organization within each of the subdivisions of the cochlear nucleus (CN), but intranuclear microstimulation will excite the axonal projections from the CN as well as the cell bodies, and also may depolarize the large dendrites that may span auditory nerve terminal representing a range of acoustic frequencies.

In previous reports, we have described a method of quantifying the ability of the intranuclear microstimulation to selectively activate the tonotopic organization of the lower auditory system, using current source-sink density analysis of the evoked

responses recorded in the contralateral inferior colliculus. The tonotopic organization of the anteroventral and posteroventral CN is preserved in the projection from the CN to the inferior colliculus as illustrated schematically in figure 2. The projection is primarily to the contralateral colliculus. The iso-frequency laminae are oriented more-or- less perpendicular to the dorsolateral-venteromedial axis of the central nucleus of the inferior colliculus (ICC) with lower acoustic frequencies represented dorsally and high frequencies represented ventrally and medially (e.g. Semple and Aitkins, 1979, Brown et al, 1997).

METHODS

We present results from the terminal experiment with cat CN152, in which the microstimulating array had been implanted in the cochlear nucleus for 195 days. In this cat, the shanks of the microstimulating array were oriented closer to the dorsal-ventral axis than in previous animals. The procedure for the terminal experiment was essentially as described in our previous quarterly report (QPR #4). The cat was anesthetized with Isoflurane and nitrous oxide, its heads fixed in a stereotaxic holder with hollow ear bars, to facilitate the delivery of acoustic stimuli. A wide craniectomy was made over the left posterior cerebral hemisphere, and the occipital pole of the cerebrum was removed by aspiration to expose the inferior colliculus. The cat was transported to a double-walled acoustic isolation room with its head still fixed in the stereotaxic holder. Throughout the remainder of the experiment, anesthesia was maintained with a mixture of 2-2.5% Isoflurane and oxygen delivered by a self-breathing apparatus. Respiration rate and end-tidal CO_2 was monitored continuously. Core body temperature was maintained at 37-39.0˚C using a circulating water heating pad. All sound-generating equipment was located outside of the sound isolation room.

Multiunit neuronal activity was recorded in the contralateral inferior colliculus using a 32-site silicon substrate probe designed and fabricated by NeuroNexus, Inc (Figure 3). The recording sites are spaced 100 μm apart over a total span of 3 mm, which is somewhat less than the span of the domestic cat's ICC along the dorsolateral-ventromedial axis (approximately 4.5 mm). The recording probe was inserted into the inferior colliculus at an angle of 45^o from the vertical, and approximately along the

tonotopic gradient. The shanks of these new probes were longer and much more flexible than those that we had used in the acute experiments described in QPR #4, and they would not penetrate through the pia overlying the inferior colliculus. The pia was carefully dissected from about 50% of the surface of the dorsal surface. This undoubtedly damaged the external nucleus, but the central nucleus of the IC (ICC) appears not to have been damaged.

Data were recorded during 3 penetrations into the IC:

Penetration	Location	Depth spanned (mm beneath surface of IC)
1	Caudal IC	1 to 4
2	Rostral IC	2 to 5
3	Caudal IC, medial to P1	2 to 5

For each penetration of the recording probe into the ICC, the response to acoustic stimuli was recorded in the ICC. Prior to this experiment, we had replaced the tweeter in our loudspeaker system with an electrostatic unit with an acoustic bandpass extending to beyond 25 kHz. Tone bursts spanning 2.6 to 26 KHz (approximately 85 db spl) and 100 ms in duration with a rise time of 10 ms were used. Neuronal activity was recorded simultaneously from alternate probe sites (16 sites, spaced 200 μm apart) using the custom hardware and computer software described in previous progress reports. The location of the sites on the microstimulating array is illustrated in figure 4. Controlled-current, biphasic stimulus pulses (150 μs/ph in duration at 50 Hz) were applied to the individual microelectrode sites in the cochlear nucleus. 1500 successive stimulus pulses were delivered in sequence at 50 Hz through microstimulating sites 2, 4,6,7,8,11,13,14,16. The stimulus current was 10, 20 and 30 μA (1.5, 3 and 4.5 nC/phase). 4.5 nC/phase is the maximum charge per phase used in previous studies to generate the response growth functions that are used to characterize the long-term stability of the chronically implanted electrodes in the cat cochlear nucleus. In the human patients implanted to date, the thresholds for auditory percepts from the penetrating microelectrodes have been 1.7 nC/phase or less . The

response to 1,500 successive stimulus pulses delivered to each microstimulating site was recorded simultaneously from 16 sites in the contralateral ICC.

Data were analyzed offline used the custom software described in previous reports. First, a common template of the compound evoked responses is generated by summing (averaging) 1500 successive responses to the microstimulation. This template then is subtracted from each individual trace (response), in order to suppress the large evoked response. Low- and high-frequency noise that is unique to each trace then is removed by broadband filtering using a passband of 1000-8000 Hz (time domain convolution filter using sinx/x kernels).

Neuronal action potentials (multi-unit activity) were detected as events that exceeded 3.5 x the rms noise level of the recordings. Post-stimulus time (pst) histograms were generated from those events. Contour ("topographic style") maps of the evoked neuronal activity were generated from the set of 16 PST histograms representing the neuronal activity recorded along the dorsolateral-ventromedial axis if the ICC. On these contour maps, the ordinant is the distance above the deepest recording site in the ICC (at the tip of the probe), and the abscissa is time after the stimulus pulse. The contour line labels represent the total number of action potentials in each of the 100 μs bins of the PST histograms from which the maps were constructed. The maxima of the response to the acoustic tones of different frequencies is indicated near the right y-axis.

Contour maps of current source-sink density also were generated from each set of 16 simultaneously-recorded templates of the averaged evoked potentials. Current source density (CSD) analysis has proven useful for localizing induced neural activity. The technique locates regions within the tissue volume in which current is passing from the extracellular compartment into (Sink) or out of (source) a spatially extensive intracellular compartment. The CSD at point x,y,z within the tissue volume represents the net current flowing in or out of the neural elements and is given by:

$$I_{d(x,y,z)} = -[\ \sigma_x\ \delta^2\ \phi/\delta x^2 + \sigma_y\ \delta^2\ \phi/\delta y^2 + \ \sigma_z\ \delta^2\ \phi/\delta z^2\ ] \quad (1)$$

where ϕ is the field potential at x,y,z, and σ_x , σ_y and σ_z are the principal tissue conductances (Freeman and Nicholson, 1975). To compute equation 1, the extracellular field potential must be measured simultaneously at 7 (or more) points, at and around x,y,z. However, in situations in which the neuronal responses to the stimulation are quite constant over time and in which the tissue is nearly isotropic ($\sigma x \cong \sigma y \cong \sigma z \cong \sigma$) as appears to be the case in the central nucleus of the inferior colliculus (Harris, 1987), then the current source density can be estimated from measurements of the averaged evoked potential obtained along a single axis. The representation of sound frequencies determined with this approach are consistent with the known organization of the central nucleus of the inferior colliculus (Harris, 1987) and very similar to the results obtained using simultaneous multi-unit analysis (McCreery et al, 1998).

Since the neuronal activity was recorded at fairly widely-spaced intervals in the ICC (200 μm), we computed the (negative of) the 2nd spatial derivative (the CSD function) as :

$$I_{d(x,y,z),} \cong D(z)= [\ \phi(x-h) - 2\phi(x) + \phi(x+h)\ ] \qquad (2)$$

Here, h is the spacing between the points at which the instantaneous field potential ϕ is measured. We did not measure the conductivity of the living tissue in the inferior colliculus, and therefore, the CSD is expressed as arbitrary units. Current sinks (negative values of CSD) occur when membrane depolarization causes ionic currents to flow into a neuron. Current sinks are commonly equated with regions of excitatory synaptic activity. Under these conditions, the spatially adjacent current sources represent the return of this current to the extracellular compartment, through passive membrane. Sinks also may be generated by synchronous action potentials, wherein the spatially adjacent current sources represent the return of the current to the extracellular compartment through passive neuronal membrane, and the temporally adjacent sources represent repolarization of the active neuronal membranes.

RESULTS

Figures 5, 6 & 7 show contour plots of the neuronal activity induced in the ICC while stimulating with various microelectrode sites of the chronically-implanted array in the contralateral cochlear nucleus. In these plots, the abscissa is the time in milliseconds after each stimulus pulse, and the ordinate is depth in the ICC, quantified on the left as μm above the deepest recording site and on the right as the depth of maximum response to acoustic tone bursts of the frequencies indicated. The contour line labels represent the total number of action potentials per 40 μs bin, for all 1,500 successive presentations of the electrical stimulation in the CN. For reference, the location of the microstimulating sites is shown in the diagram at the bottom of each page. In penetration 1, in the caudal IC, there was considerable spontaneous neuronal activity deep in the IC. This spontaneous activity is distributed uniformly along the abscissa and appears as horizontal bands in the contour maps. In contrast, the activity evoked by the microstimulation in the CN occurred 4 to 6 ms after each stimulus pulse, and therefore appears in the contour maps as “patches”.

Most of the microstimulating sites in the CN activated neurons in the ICC over a range of depths, but the activity from any one stimulating sites corresponded to a fairly narrow range of acoustic frequencies, even at the maximum stimulus amplitude of 30 μA (4.5 nC/ph). Collectively, the responses span a wide range of acoustic frequencies, from about 2 KHz to above 20 KHz. The responses appear to be most clearly represented in the data from penetration #2, which was in the rostral-medial part of the IC (Figure 6A, B).

It is notable that adjacent microstimulating sites in the medial part of the CN separated by only 300 μm (sites 4 & 8, and also sites 2 & 6) induced neuronal activity that was largely non-overlapping along the dorsolateral-ventromedial of the ICC, even at the highest stimulus amplitude of 30 μA. Overall, the neuronal activity evoked in the IC from the different sites in the CN is consistent with the known tonotopic organization of the ventral CN, with low frequencies represented in the ventral part of the nucleus. The only exception was microstimulating electrode 13, which was very shallow in the CN and also induced multiunit activity shallow in the IC. Since the shanks on the

stimulating array were oriented in a dorsolateral-to-ventromedial direction (so that the underside of the array could lie on the sloping dorsolateral surface of the CN), the lateral shanks tended to be more ventral in the CN, and thus a site on the lateral shank (e.g., site 7) would be expected to activate neurons in the cochlear nucleus that corresponds to lower acoustic frequencies than would the corresponding site on the medial shank (e.g., site 6), and thus should excite activity shallower in the IC. This indeed is what is seen.

Figure 8 shows the set of averaged evoked potentials (displayed as a set of stacked plots and also as a contour plot) recorded from each of the 16 electrode sites in the IC during penetration 2, while stimulating in the CN with electrode site 6. Also shown is the density of the multiunit activity, and a contour plot of the current sink density, as computed from the set of evoked potentials, according to equation (2). The contour plots of the current sink density span 30% to 100% of the maximum (negative) value of the current sink, in increments of 10% of the maximum. This representation was chosen to best illustrate the correspondence between the current sink density and the neuronal activity. It is notable that little multi-unit activity was recorded between 3 and 5 ms after each stimulus pulse, when the amplitude of the evoked potentials was greatest. However, the maxima of the current sink density and the maximum density of the multi-unit activity both occurred about 6 ms after the stimulus pulse. Note however, that the maximum current sink density in the IC was about 300 μm dorsolateral of the depth of greatest multiunit activity.

Figure 9A,B,C,D show the density of the multiunit neuronal activity (left panel) and the corresponding current sink density, recorded during penetration 2, for 5 of the microstimulating sites in the CN. In all cases, there is excellent correspondence between the post-stimulus time of the maximum multiunit activity and the maximum current sink density. In contract, the maximum of the evoked potentials did not consistently correspond in depth or in time with the neuronal activity, However, when the maximum response was in the ventral or the ventromedial IC, the maxima of the current sinks were 200 to 300 μm shallower (more dorsolateral) in the IC than the maximum multiunit activity.

DISCUSSION

We have demonstrated and compared two techniques for quantifying the ability of a chronically implanted central auditory prosthesis to selectively activate different information channels, using stimulus parameters that are clinically relevant. Both approaches (maps of the spatial-temporal density of multi-unit activity in the ICC and spatial-temporal density of current sinks in the ICC) give similar results, but the current sinks were slightly dorsolateral of the maxima of the multiunit activity. This shift could be an artifact of the multi-site recording probe, These are quite broad at the top and taper towards the tip, and the multiunit activities from the sites that are closer to the tip (deeper in the IC) tend to have better signal-to-noise ratios. This would cause the centroids of the maps of the density of the multiunit activity to be shifted deeper in the ICC, since only neuronal units with S/N greater than 3.5 x the RMS noise level were counted.

We have yet to determine the best way to integrate the information from of the multiunit and current sink density methods, and how each approach might complement the other. The approach based on multiunit activity is biased towards the large neurons that tend to give greater S/N, but this probably is true also of the current sink density analysis. The source-sink density also will emphasize neuronal activity that is better synchronized, but should reveal activity from small neurons and axons, provided they are numerous, there is some synchrony in their activity, and the intracellular compartment is spatially extensive (i.e, they have elongated processes, such as axons). If recording probes can be developed that consistently record actions potentials with the signal-to-noise ratios that are sufficient for reliable spike sorting, then the unit recording could be used to separate the contributions of different neurons, and perhaps different functional classes of neurons in the ICC; information that is may not be available from the current sink density analyses.

REFERENCES CITED

M. Brown, W.R Webster and R.L, Martin, “ The three-dimensional frequency organization of the inferior colliculus of the cat: a 2-deoxyglucose study”. *Hearing Research vol. 104 pp 57-73,* 1997.

J. A. Freeman and C. Nicholson, "Experimental optimization of current source-density technique for anuran cerebellum," *J Neurophysiol*, vol. 38, pp. 369-82., 1975

D. M. Harris, "Current source density analysis of frequency coding in the inferior colliculus," *Hear Res*, vol. 25, pp. 257-66, 1987.

P.A. Leake and R.L Snyder. “Topographic organization of the central projections of the spiral ganglion in cats,” *J Comp Neurol*, vol. 281, pp. 612-629, 1989

D. B. McCreery, R. V. Shannon, J. K. Moore, and M. Chategee, "Accessing the tonotopic organization of the ventral cochlear nucleus by intranuclear microstimulation," *IEEE Transactions on Rehabilitation Engineering*, vol. 23, pp. 391-399, 1998.

M.N. Semple and L.M. Aitkins. “ Representation of sound frequencies and laterality by units in the central nucleus of cat inferior colliculus”, *J. Neurophysiology, vol. 42 pp. 1629-1639, 1979*

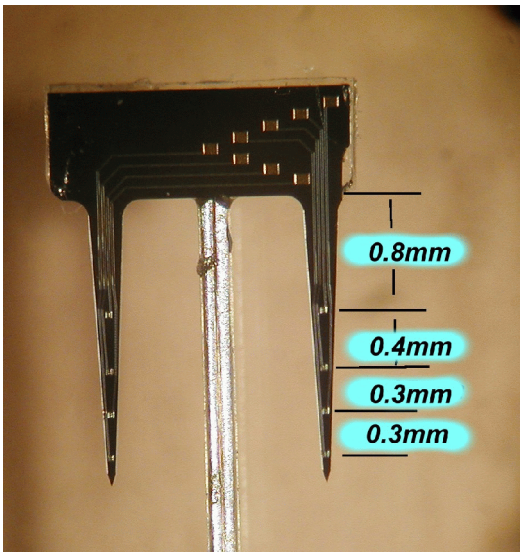

Figure 1A

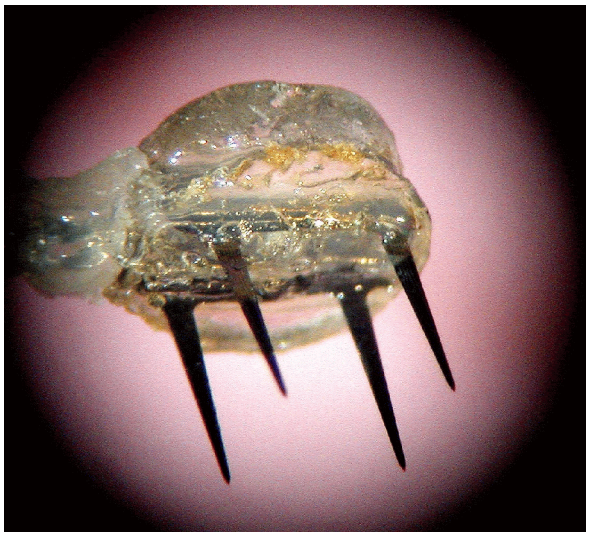

Figure 1B

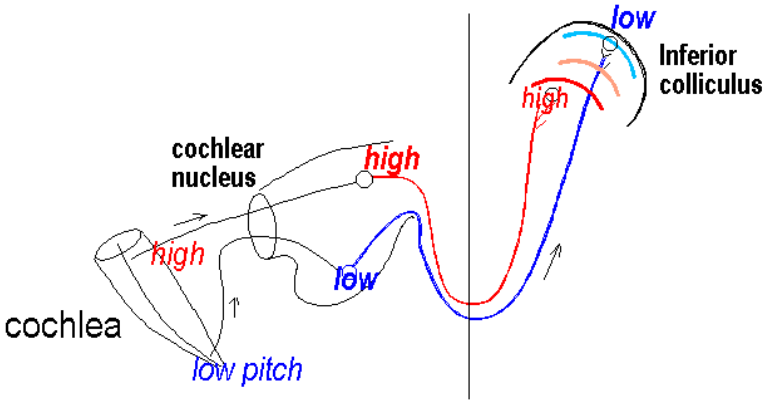

Figure 2

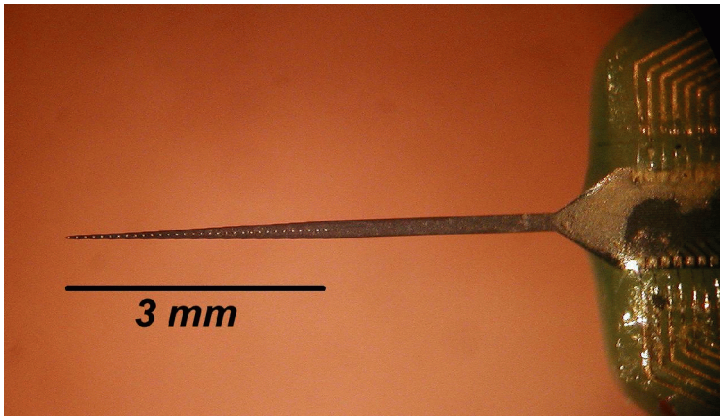

Figure 3

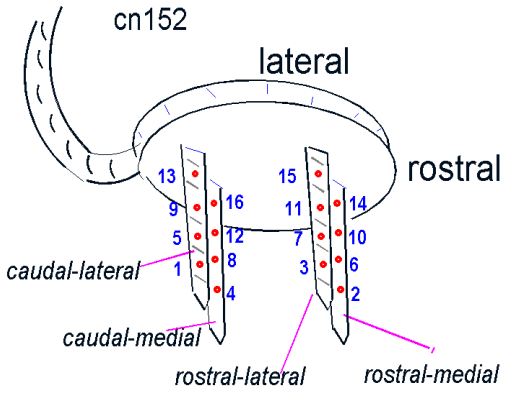

Figure 4

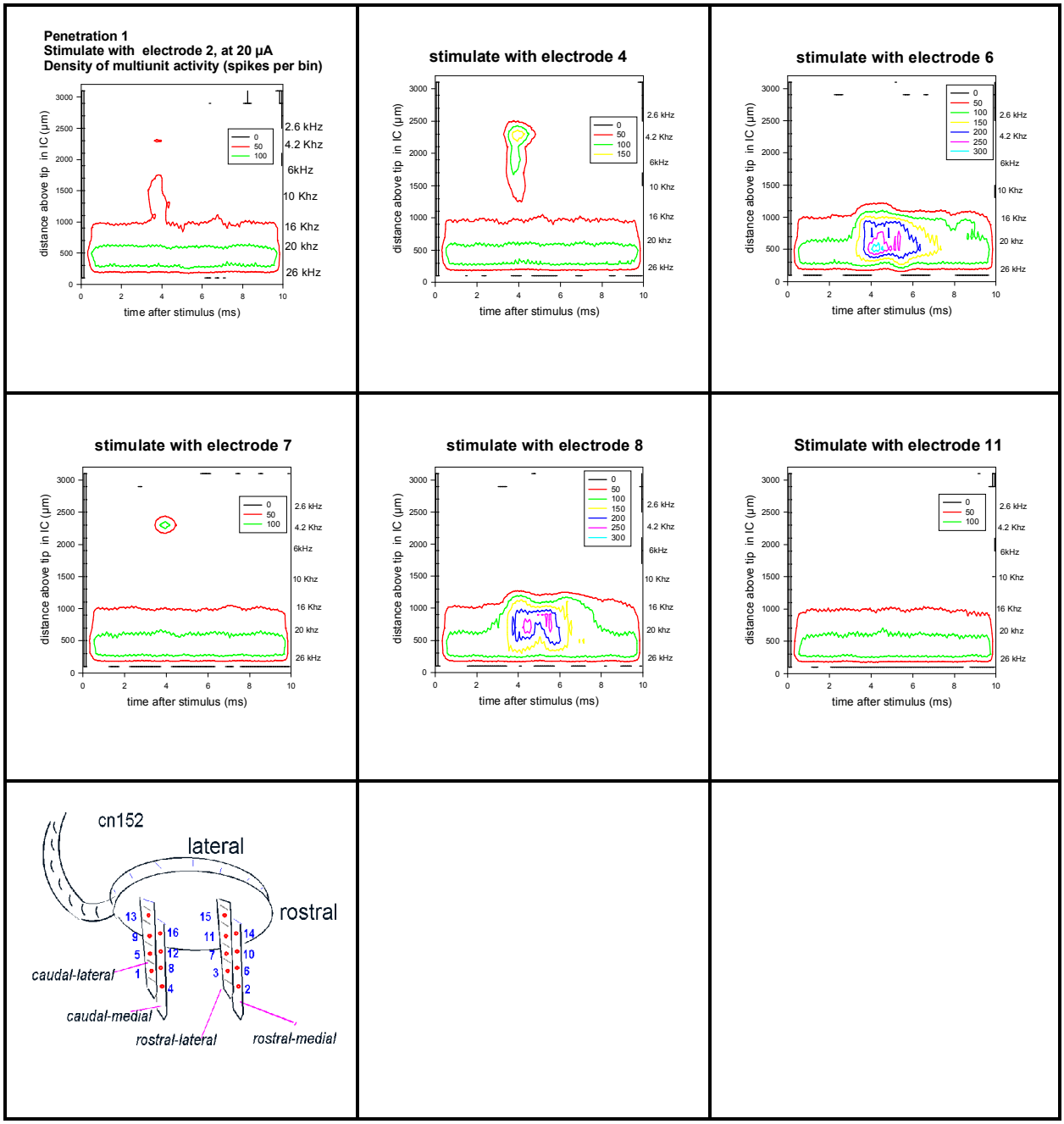

Figure 5A Density of multiunit activity in the ICC. Penetration 1, 20 µA

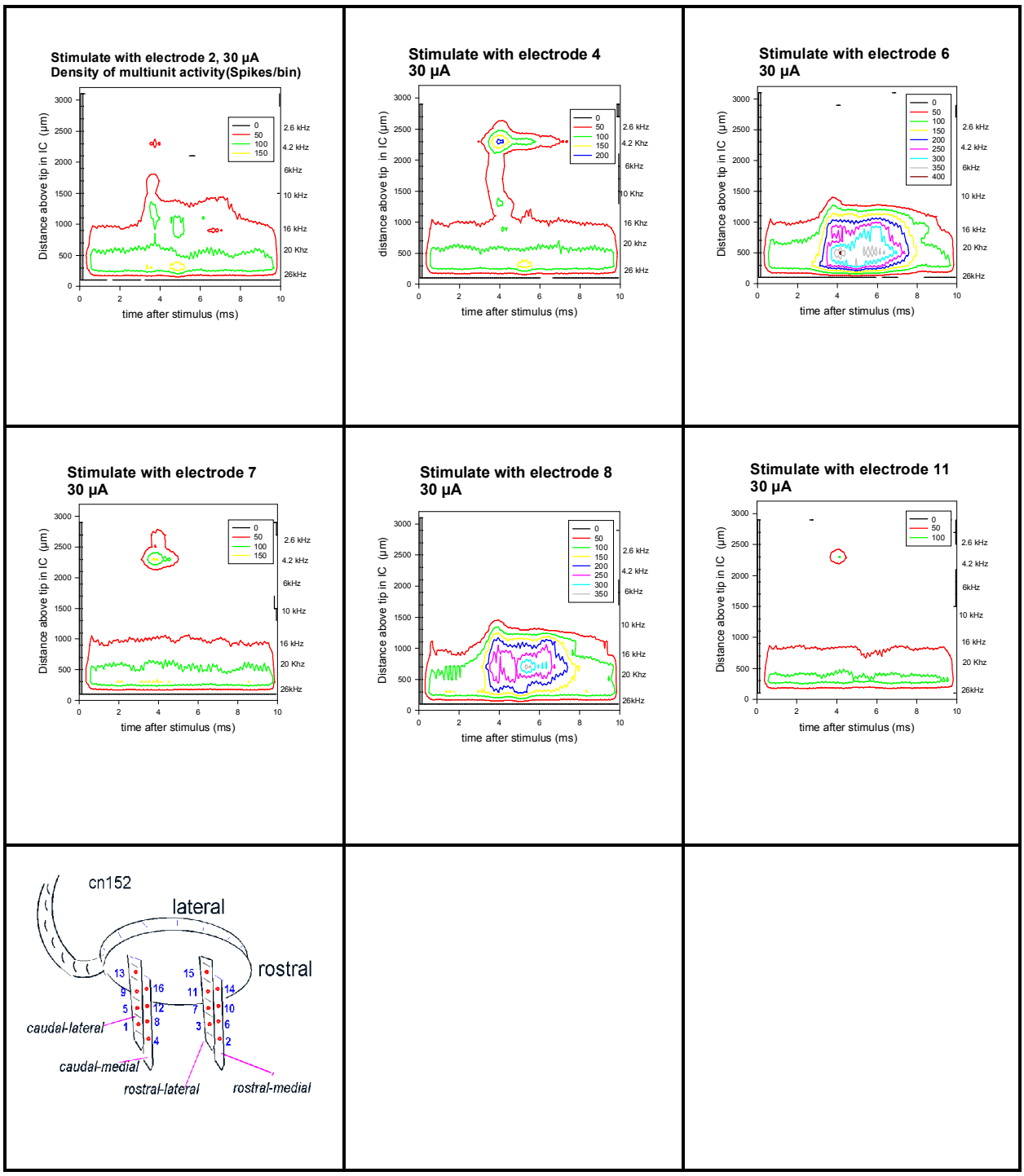

Figure 5B- Density of multiunit activity. Penetration 1, 30 µA

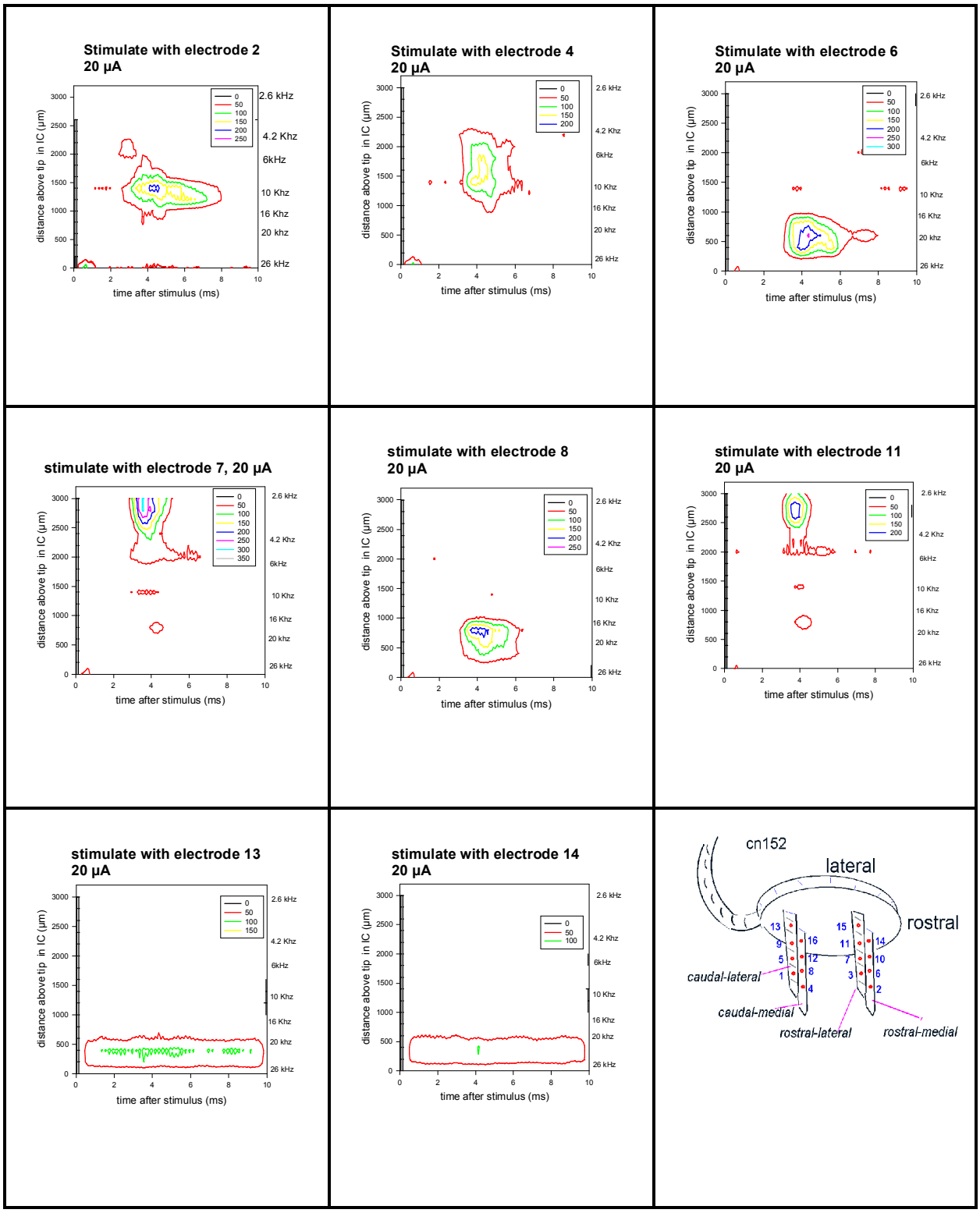

Figure 6A. Density of multiunit activity. Penetration 2, 20 µA

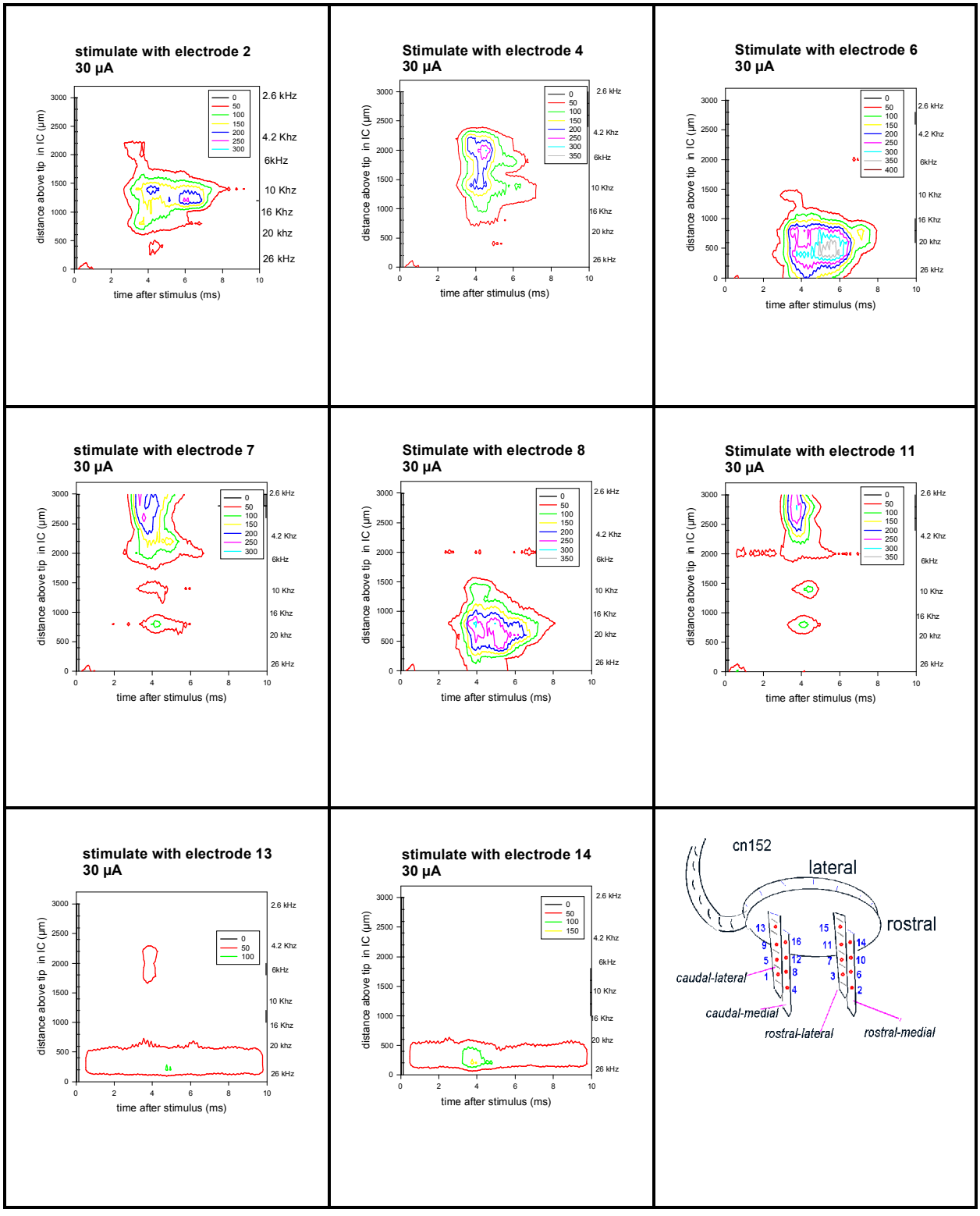

Figure 6B Density of multiunit activity. Penetration 2, 30 µA

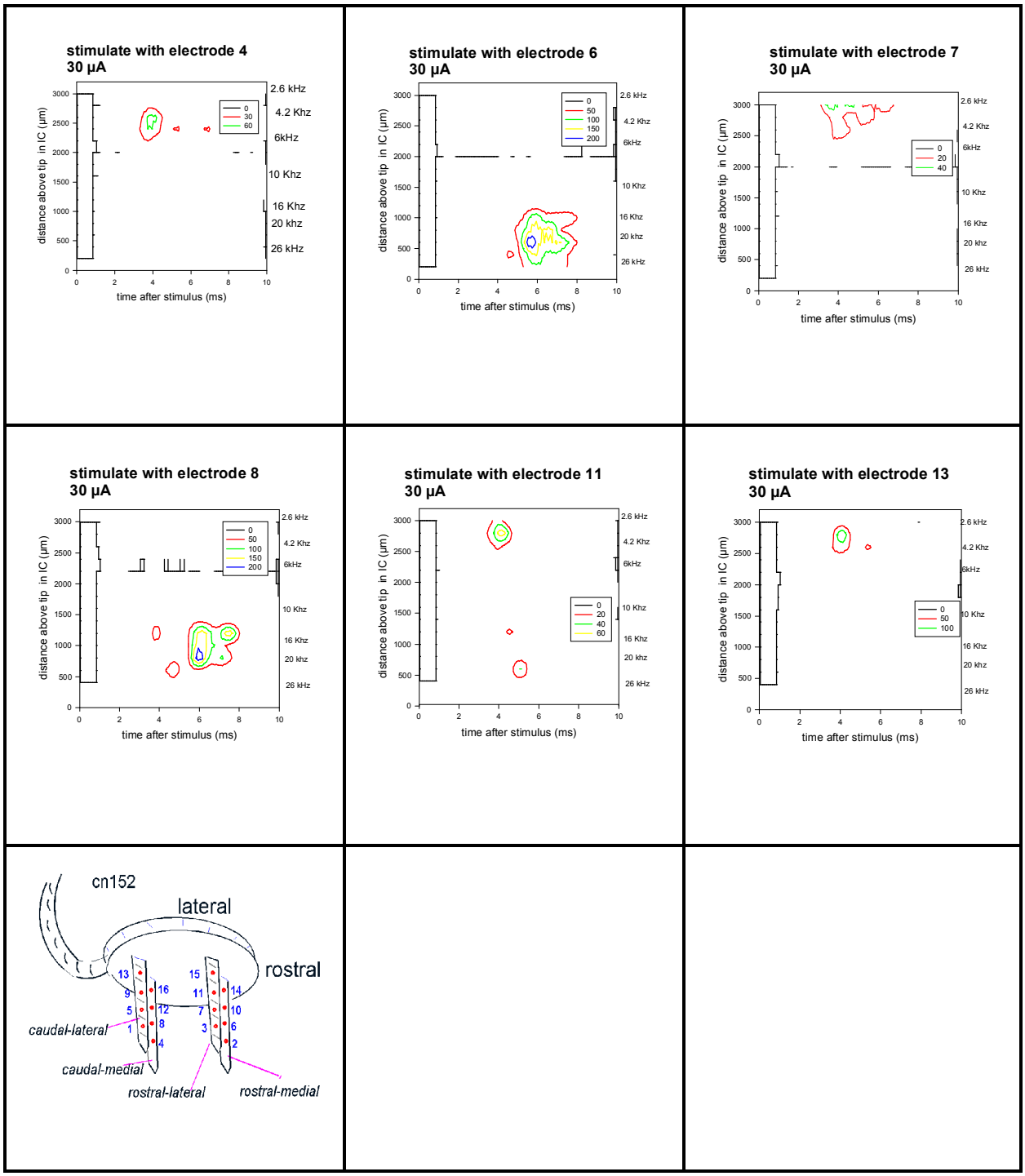

Figure 7 Density of multiunit activity. Penetration 3; 30 µA

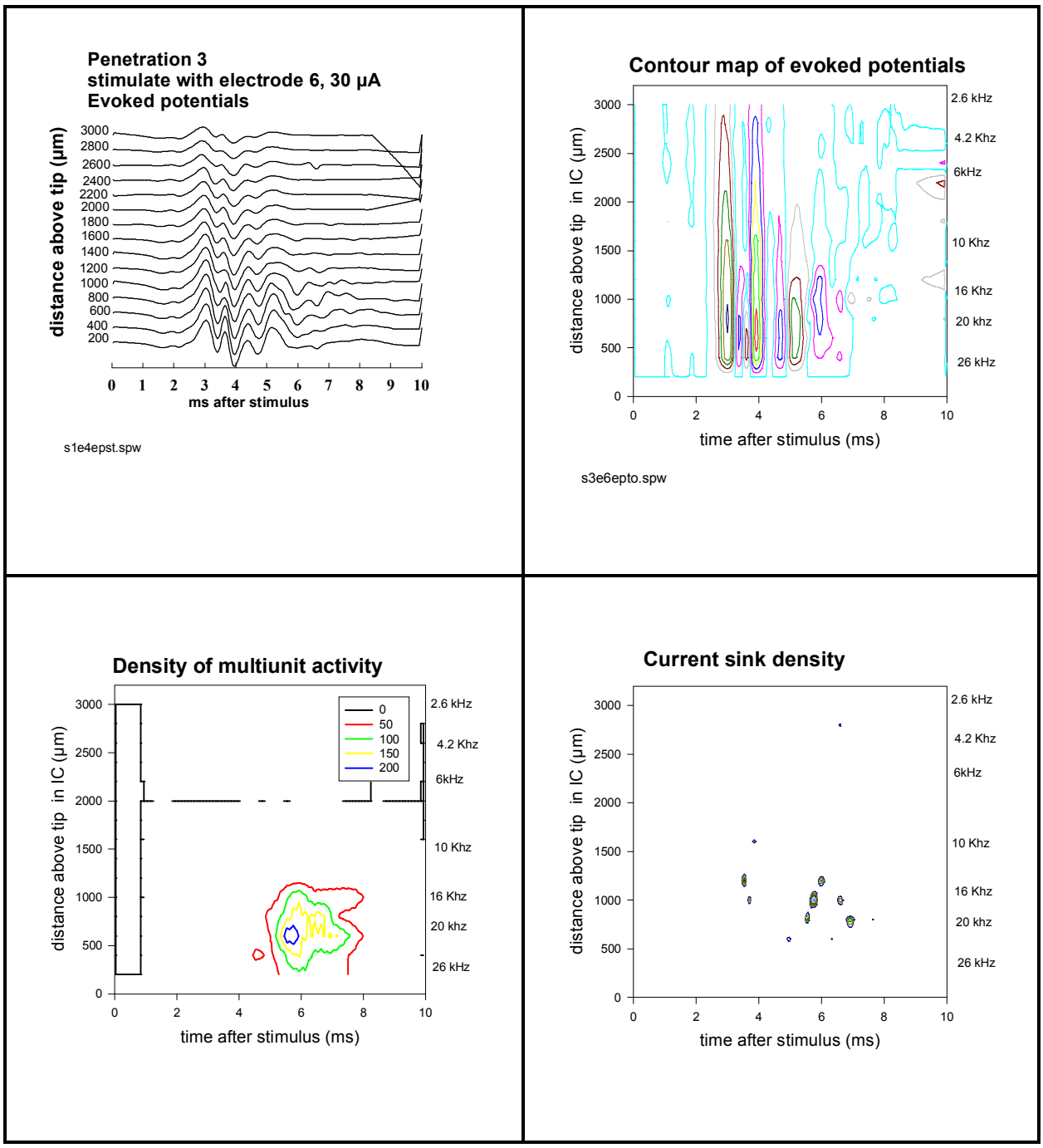

Figure 8 Comparison of evoked potentials, density of action potentials and current sink density (penetration 3)

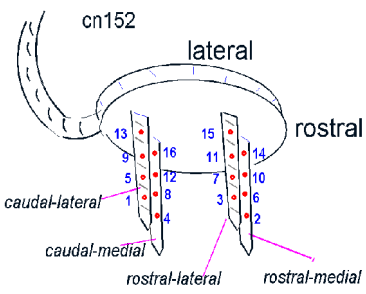

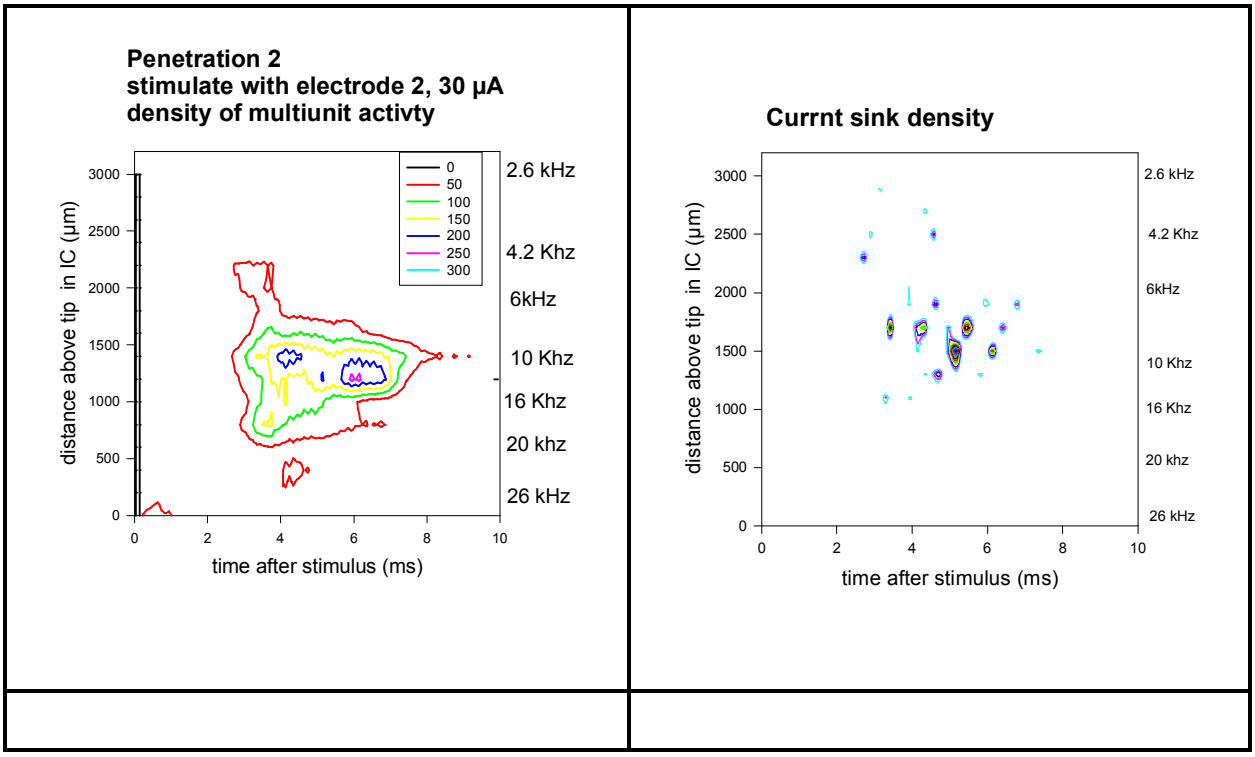

Figure 9A Comparisons of density of action potentials and current sink density for penetration 2

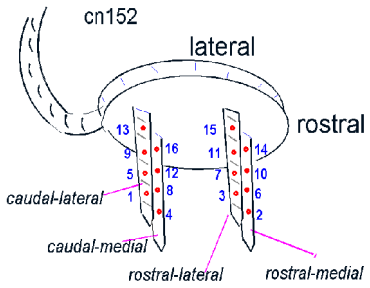

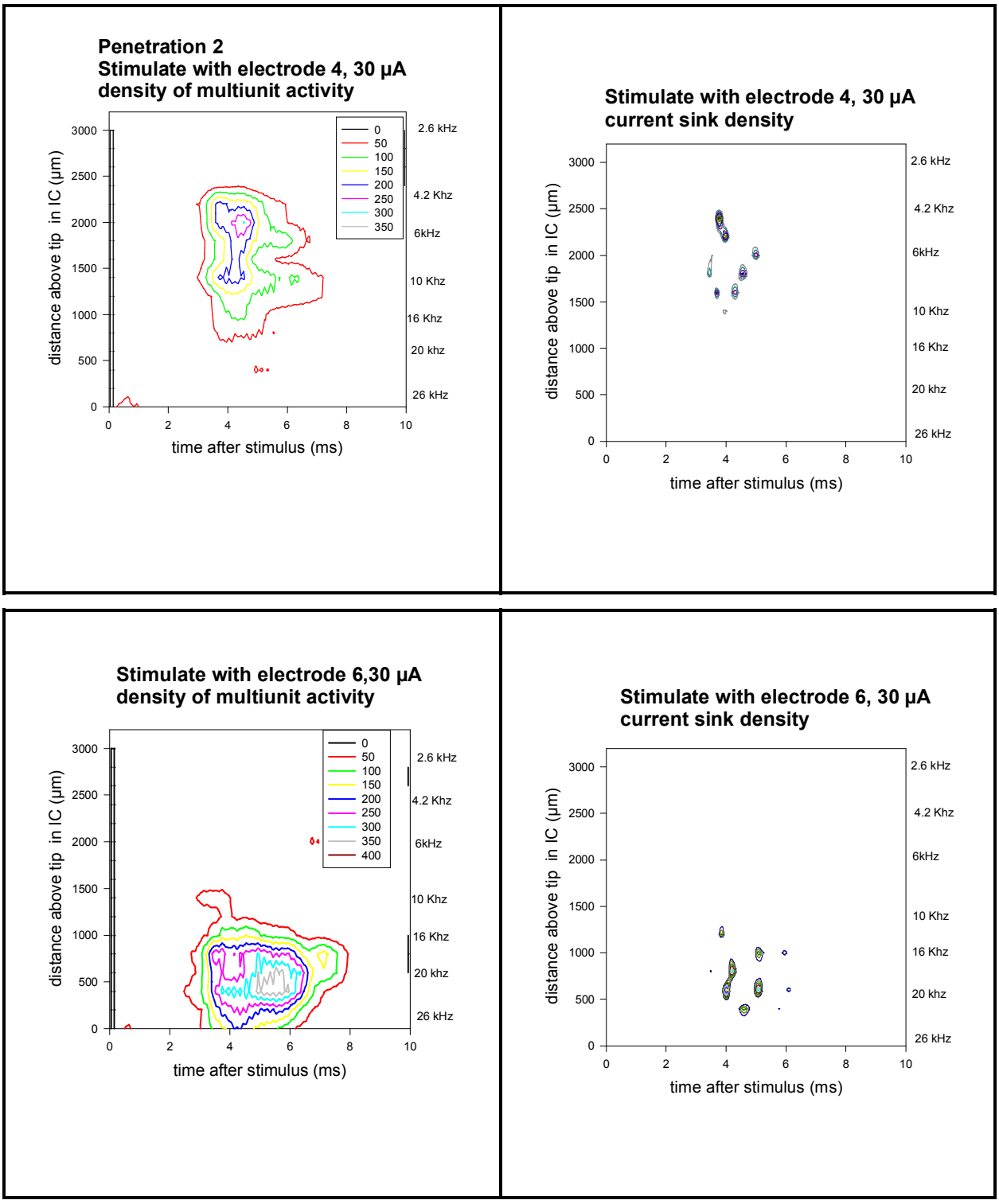

Figure 9B Comparisons of density of action potentials and current sink density for penetration 2 (continued)

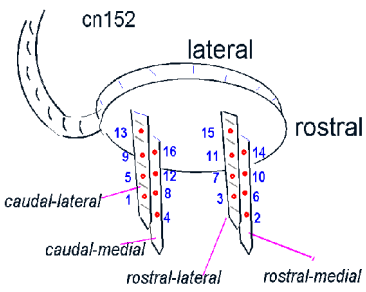

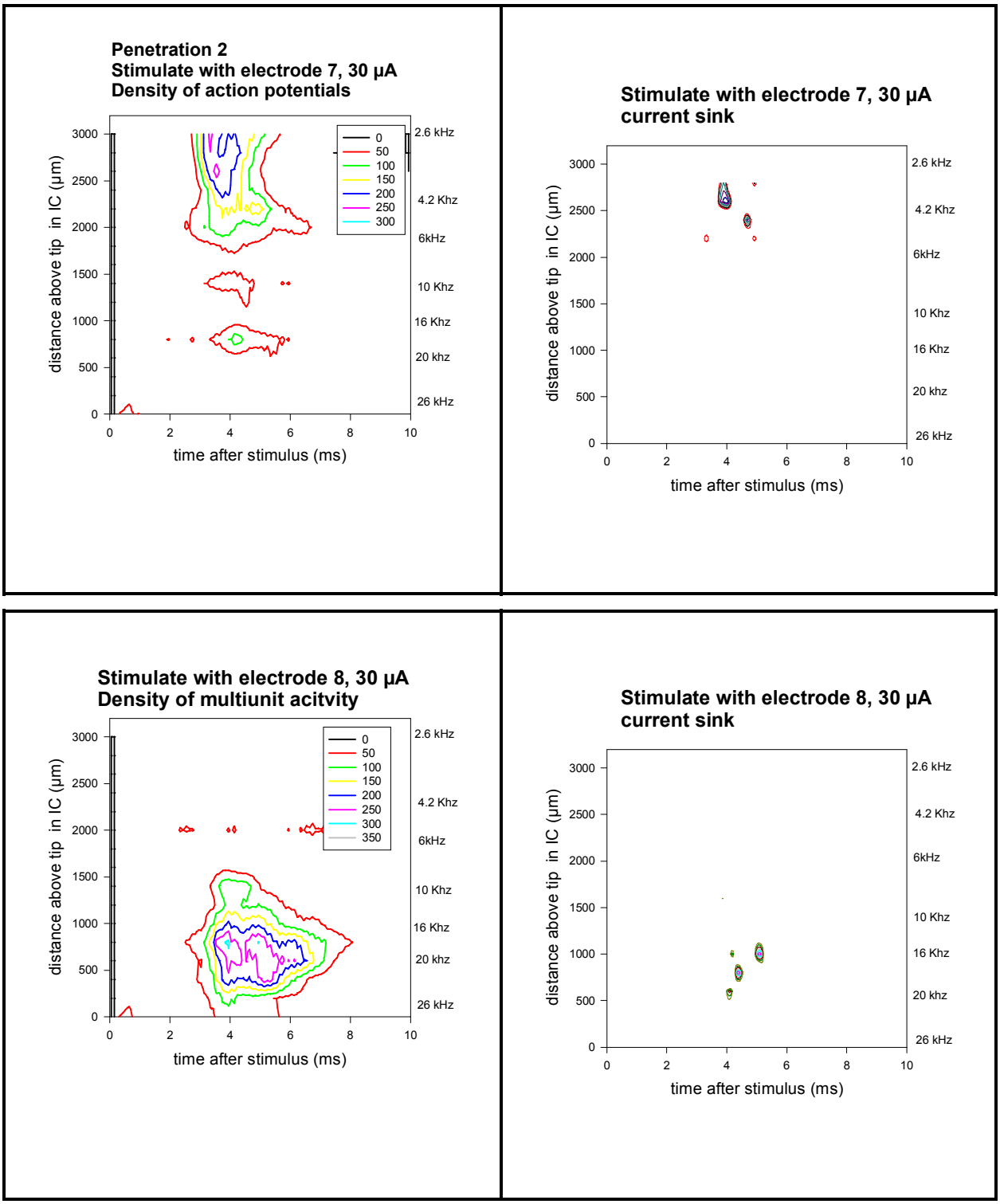

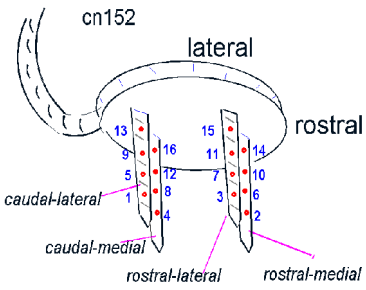

Figure 9C Comparisons of density of action potentials and current sink density for penetration 2 (continued)

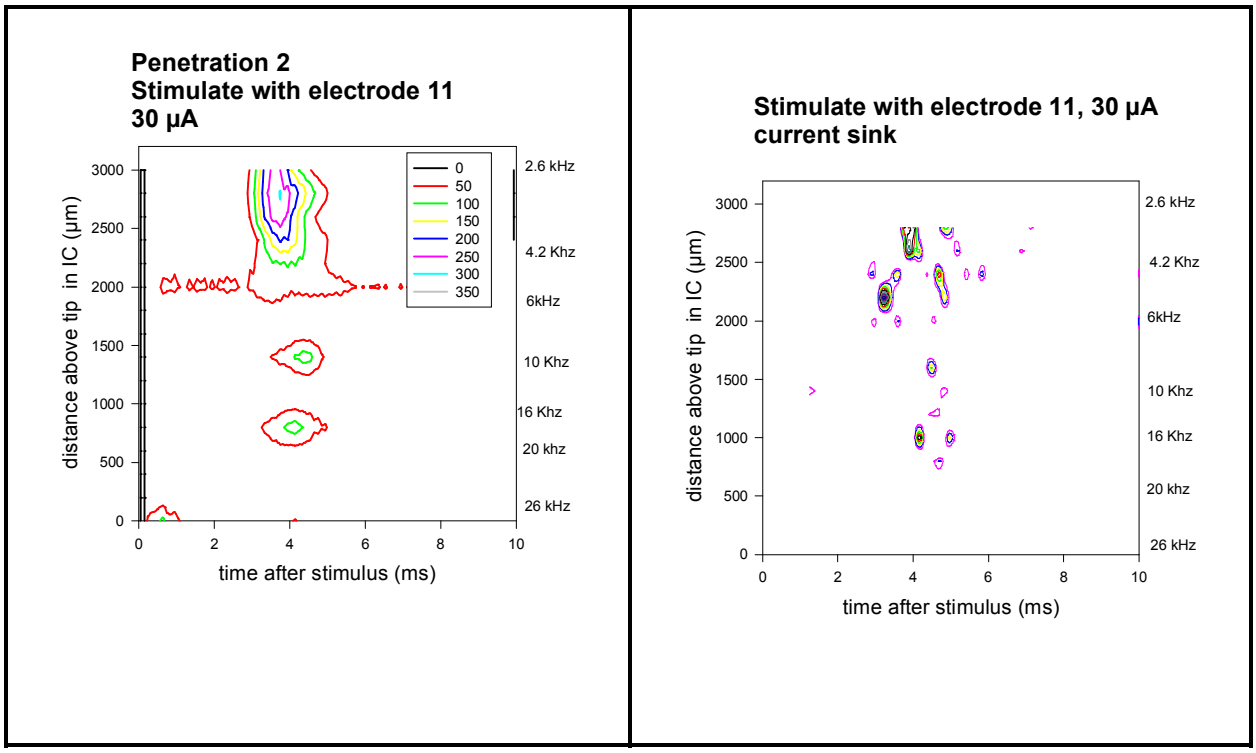

Figure 9D Comparisons of density of action potentials and current sink density for penetration 2 (continued)